

EXTRACTING $\sigma_{\pi N}$ FROM PIONIC ATOMS*

ELIAHU FRIEDMAN, AVRAHAM GAL

Racah Institute of Physics, The Hebrew University, Jerusalem 91904, Israel

(Received October 7, 2019)

We discuss a recent extraction of the πN σ term $\sigma_{\pi N}$ from a large-scale fit of pionic-atom strong-interaction data across the periodic table. The value thus derived, $\sigma_{\pi N}^{\text{FG}} = 57 \pm 7$ MeV, is directly connected via the Gell-Mann–Oakes–Renner expression to the medium-renormalized πN isovector scattering amplitude near threshold. It compares well with the value derived recently by the Bern–Bonn–Jülich group, $\sigma_{\pi N}^{\text{RS}} = 58 \pm 5$ MeV, using the Roy–Steiner equations to control the extrapolation of the vanishingly small near-threshold πN isoscalar scattering amplitude to zero pion mass.

DOI:10.5506/APhysPolB.51.45

1. IntroductionThe πN σ term

$$\sigma_{\pi N} = \frac{\bar{m}_q}{2m_N} \sum_{u,d} \langle N | \bar{q}q | N \rangle, \quad \bar{m}_q = \frac{1}{2}(m_u + m_d), \quad (1)$$

sometimes called the nucleon σ term σ_N , records the contribution of explicit chiral symmetry breaking to the nucleon mass m_N arising from the non-zero value of the u and d quark masses in QCD. Early calculations yielded a wide range of values, $\sigma_{\pi N} \sim 20\text{--}80$ MeV [1]. Recent calculations use two distinct approaches: (i) pion–nucleon low-energy phenomenology guided by chiral EFT, with or without solving Roy–Steiner equations, result in values of $\sigma_{\pi N} \sim 50\text{--}60$ MeV [2–6], the most recent of which is 58 ± 5 MeV; and (ii) lattice QCD (LQCD) calculations reach values of $\sigma_{\pi N} \sim 30\text{--}50$ MeV [7–13], the most recent of which is 41.6 ± 3.8 MeV. This dichotomy is demonstrated in the left panel of Fig. 1. However, when augmented by chiral perturbation expansions, LQCD calculations reach also values of ~ 50 MeV, see *e.g.* Refs. [14–17]. Ambiguities in chiral extrapolations of LQCD calculations to the physical pion mass are demonstrated in the right panel of Fig. 1.

* Presented by A. Gal at the 3rd Jagiellonian Symposium on Fundamental and Applied Subatomic Physics, Kraków, Poland, June 23–28, 2019.

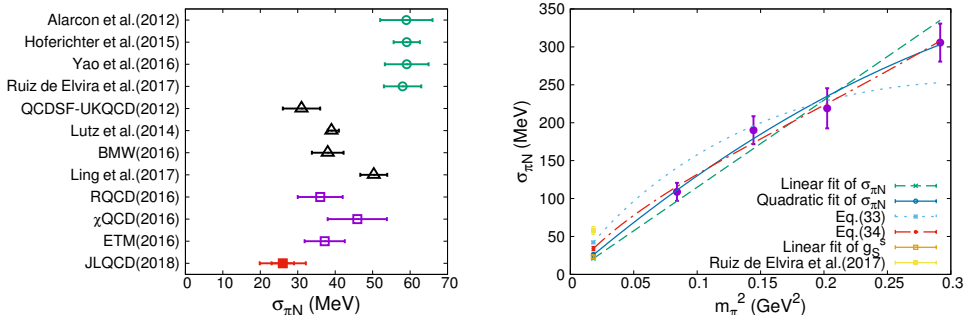


Fig. 1. (Color online) Left: values of $\sigma_{\pi N}$ from recent calculations, based on πN phenomenology (upper right/green) and in LQCD (other colors). Right: chiral extrapolations of LQCD derived $\sigma_{\pi N}$ values to the physical pion mass. Figure adapted from JLQCD (2018) work [12].

A third approach for evaluating $\sigma_{\pi N}$ was recently proposed by us [18] focusing on the $\sigma_{\pi N}$ -dependent in-medium renormalization of the πN isovector scattering length b_1 , determined from a wealth of strong-interaction level shifts and widths data in pionic atoms across the periodic table [19]. This contrasts with extrapolating the vanishingly small πN isoscalar scattering length b_0 from $m_\pi \approx 138$ MeV to the Cheng–Dashen point or nearby at $m_\pi \sim 0$, as done in the first approach. To demonstrate the issues involved in comparing these two methodologies, we cite from a recent work by the Bern–Bonn–Jülich group [20] an expression relating the expected departure of the evaluated $\sigma_{\pi N}$ from their value of 59 ± 3 MeV [4] upon varying the input values of b_0 and b_1

$$\sigma_{\pi N} \approx (59 \pm 3) \text{ MeV} + 1.116 \Delta b_0^{\text{free}} + 0.390 \Delta b_1^{\text{free}}, \quad (2)$$

where Δb_j^{free} , $j = 0, 1$, is the difference between the values of b_j^{free} (in units of $10^{-3} m_\pi^{-1}$) used in a given specific model and those used in the calculation of Ref. [4]. Equation (2) suggests that the uncertainty in the determination of $\sigma_{\pi N}$ incurred by the model dependence of b_0^{free} is roughly three times larger than that incurred by the model dependence of b_1^{free} . Regarding the model dependence of these free-space scattering lengths, we note the two sets of input scattering lengths ($b_0^{\text{free}}, b_1^{\text{free}}$) discussed in Ref. [20]

$$(-0.9, -85.3) \times 10^{-3} m_\pi^{-1}, \quad (+7.9, -85.4) \times 10^{-3} m_\pi^{-1}, \quad (3)$$

differing from each other by whether or not charge-dependent effects are incorporated into the values of scattering lengths derived from $\pi^- \text{H}$ and $\pi^- d$ atoms by Baru *et al.* [21]. It is evident that the charge dependence

of the near-threshold πN interaction affects dominantly the isoscalar b_0^{free} while leaving the isovector b_1^{free} basically intact. This makes an approach based on b_1^{free} quite attractive.

To set the stage for how the third approach works, we note that the πN scattering lengths [21] are well-approximated by the Tomozawa–Weinberg leading-order (LO) chiral limit [22]

$$b_0^{\text{LO}} = 0, \quad b_1^{\text{LO}} = -\frac{\mu_{\pi N}}{8\pi f_\pi^2} = -79 \times 10^{-3} m_\pi^{-1}, \quad (4)$$

where $\mu_{\pi N}$ is the πN reduced mass and $f_\pi = 92.2$ MeV is the free-space pion decay constant. This expression for the isovector amplitude b_1 suggests that its in-medium renormalization is directly connected to that of f_π , given to first order in the nuclear density ρ by the Gell-Mann–Oakes–Renner (GMOR) expression [23]

$$\frac{f_\pi^2(\rho)}{f_\pi^2} = \frac{\langle \bar{q}q \rangle_\rho}{\langle \bar{q}q \rangle} \simeq 1 - \frac{\sigma_{\pi N}}{m_\pi^2 f_\pi^2} \rho, \quad (5)$$

where $\langle \bar{q}q \rangle_\rho$ stands for the in-medium quark condensate. The decrease of $\langle \bar{q}q \rangle_\rho$ with density in Eq. (5) marks the leading low-density behavior of the order parameter of the spontaneously broken chiral symmetry. Recalling the f_π dependence of b_1^{LO} in Eq. (4), Eq. (5) suggests the following density dependence for the in-medium b_1 :

$$b_1 = b_1^{\text{free}} \left(1 - \frac{\sigma_{\pi N}}{m_\pi^2 f_\pi^2} \rho \right)^{-1}. \quad (6)$$

In this model, introduced by Weise [24, 25], the explicitly density-dependent $b_1(\rho)$ of Eq. (6) figures directly in the pion–nucleus s-wave near-threshold potential. Studies of pionic atoms [26] and low-energy pion–nucleus scattering [27, 28] confirmed that the πN isovector s-wave interaction term is indeed renormalized in agreement with Eq. (6). It is this in-medium renormalization that brings in $\sigma_{\pi N}$ to the interpretation of pionic-atom data. However, the value of $\sigma_{\pi N}$ was held fixed around 50 MeV in these studies, with no attempt to determine its optimal value.

In our recent work [18], we kept to the πN isovector s-wave amplitude b_1 renormalization given by Eq. (6), but varied also $\sigma_{\pi N}$ in fits to a comprehensive set of pionic atoms data across the periodic table. Other real πN interaction parameters varied together with $\sigma_{\pi N}$ converged at expected free-space values. Holding these parameters fixed at the converged values, except for the tiny isoscalar s-wave single-nucleon amplitude b_0 which is renormalized primarily by a double-scattering term (see below), we obtained a best-fit

value of $\sigma_{\pi N}^{\text{FG}} = 57 \pm 7$ MeV. A more comprehensive discussion of our fits to pionic atoms data is provided here. The pionic atoms approach used by us to extract $\sigma_{\pi N}$ is reviewed in the next section, followed by results and discussion in subsequent sections.

2. Pionic atoms optical potentials

The starting point in our most recent optical-potential analysis of pionic atoms [26] is the in-medium pion self-energy $\Pi(E, \vec{p}, \rho)$ that enters the in-medium pion dispersion relation

$$E^2 - \vec{p}^2 - m_\pi^2 - \Pi(E, \vec{p}, \rho) = 0, \quad (7)$$

where \vec{p} and E are the pion momentum and energy, respectively, in nuclear matter of density ρ . The resulting pion–nuclear optical potential V_{opt} , defined by $\Pi(E, \vec{p}, \rho) = 2EV_{\text{opt}}$, enters the near-threshold pion wave equation

$$[\nabla^2 - 2\mu(B + V_{\text{opt}} + V_C) + (V_C + B)^2] \psi = 0, \quad (8)$$

where $\hbar = c = 1$. Here μ is the pion–nucleus reduced mass, B is the complex binding energy, V_C is the finite-size Coulomb interaction of the pion with the nucleus, including vacuum-polarization terms, all added according to the minimal substitution principle $E \rightarrow E - V_C$. Interaction terms negligible with respect to $2\mu V_{\text{opt}}$, *i.e.* $2V_C V_{\text{opt}}$ and $2B V_{\text{opt}}$, are omitted. We use the Ericson–Ericson form [29]

$$2\mu V_{\text{opt}}(r) = q(r) + \vec{\nabla} \cdot \left(\frac{\alpha_1(r)}{1 + \frac{1}{3}\xi\alpha_1(r)} + \alpha_2(r) \right) \vec{\nabla}, \quad (9)$$

with s-wave part $q(r)$ and p-wave part, $\alpha_1(r)$ and $\alpha_2(r)$, given by [19]

$$\begin{aligned} q(r) = & -4\pi \left(1 + \frac{\mu}{m_N} \right) \{ b_0 [\rho_n(r) + \rho_p(r)] + b_1 [\rho_n(r) - \rho_p(r)] \} \\ & -4\pi \left(1 + \frac{\mu}{2m_N} \right) 4B_0 \rho_n(r) \rho_p(r), \end{aligned} \quad (10)$$

$$\alpha_1(r) = 4\pi \left(1 + \frac{\mu}{m_N} \right)^{-1} \{ c_0 [\tilde{\rho}_n(r) + \tilde{\rho}_p(r)] + c_1 [\tilde{\rho}_n(r) - \tilde{\rho}_p(r)] \}, \quad (11)$$

$$\alpha_2(r) = 4\pi \left(1 + \frac{\mu}{2m_N} \right)^{-1} 4C_0 \tilde{\rho}_n(r) \tilde{\rho}_p(r), \quad (12)$$

augmented by p-wave angle-transformation terms of the order $O(m_\pi/m_N)$. Here, ρ_n and ρ_p are neutron and proton density distributions normalized to

the number of neutrons N and number of protons Z , respectively, and $\tilde{\rho}_n$ and $\tilde{\rho}_p$ are obtained from ρ_n and ρ_p by folding a $\pi N\Delta$ form factor [30]. The coefficients b_0 , b_1 in Eq. (10) are effective density-dependent pion–nucleon isoscalar and isovector s-wave scattering amplitudes, respectively, evolving from the free-space scattering lengths, and are essentially real near threshold. Similarly, the coefficients c_0 , c_1 in Eq. (11) are effective p-wave scattering amplitudes which, since the p-wave part of V_{opt} acts mostly near the nuclear surface, are close to the free-space scattering volumes provided $\xi = 1$ is applied in the Lorentz–Lorenz renormalization of α_1 in Eq. (9). The parameters B_0 and C_0 represent multi-nucleon absorption and, therefore, have an imaginary part. Their real parts stand for dispersive contributions which often are absorbed into the respective single-nucleon amplitudes [31]. Below, we focus on the s-wave part $q(r)$ of V_{opt} .

Regarding the isoscalar amplitude b_0 , since the free-space value b_0^{free} is exceptionally small, it is customary in the analysis of pionic atoms to supplement it by double-scattering contributions induced by Pauli correlations. For completeness, we also include similar contributions to b_1 which decrease its value, although by only less than 10%. Thus, the single-nucleon b_0 and b_1 terms in Eq. (10) are extended to account also for double-scattering [29, 32]

$$\tilde{b}_0 \rightarrow \tilde{b}_0 - \frac{3}{2\pi} \left(\tilde{b}_0^2 + 2\tilde{b}_1^2 \right) p_{\text{F}}, \quad \tilde{b}_1 \rightarrow \tilde{b}_1 + \frac{3}{2\pi} \left(\tilde{b}_1^2 - 2\tilde{b}_0\tilde{b}_1 \right) p_{\text{F}}, \quad (13)$$

where $\tilde{b}_j \equiv (1 + \frac{m_\pi}{m_N})b_j$, and p_{F} is the local Fermi momentum corresponding to the local nuclear density $\rho = 2p_{\text{F}}^3/(3\pi^2)$.

Regarding the isovector amplitude b_1 , it affects primarily level shifts in pionic atoms with $N - Z \neq 0$. However, it affects also $N = Z$ pionic atoms through the dominant quadratic b_1 contribution to b_0 of Eq. (13). This dominance follows already at the level of b_1^{free} from a systematic expansion of the pion self-energy up to $O(p^4)$ in nucleon and pion momenta within chiral perturbation theory [33]. Following Ref. [34], it can be argued that it is the in-medium b_1 Eq. (6) that enters the Pauli-correlation double-scattering contribution in Eq. (13). This approach has been practised in numerous global fits to pionic atoms by us [19, 26] as well as by other groups, *e.g.* Geissel *et al.* [35], using a fixed value of $\sigma_{\pi N}$. To study the role of a variable $\sigma_{\pi N}$ as per Eq. (6), we extended b_1 wherever appearing in Eq. (13) by substituting

$$b_1 \rightarrow b_1 \left(1 - \frac{\sigma_{\pi N}}{m_\pi^2 f_\pi^2 \rho} \right)^{-1}. \quad (14)$$

Regarding the nuclear densities ρ_p and ρ_n that enter the potential, Eqs. (10)–(12), two-parameter Fermi distributions with the same diffuseness parameter for protons and neutrons were used [19, 36] yielding lower values

of χ^2 than other shapes do for pions. With proton densities determined from nuclear charge densities, the neutron densities were varied, searching for best agreement with the pionic atoms data by assuming a linear dependence of $r_n - r_p$, the difference between the root-mean-square (r.m.s.) radii, on the neutron excess ratio $(N - Z)/A$

$$r_n - r_p = \gamma \frac{N - Z}{A} + \delta, \quad (15)$$

with γ close to 1.0 fm and δ close to zero. Here, we used $\delta = -0.035$ fm and varied γ . For example, $\gamma = 1$ fm means $r_n - r_p = 0.177$ fm in ^{208}Pb , a value compatible with several analyses of pion strong and electromagnetic interactions in ^{208}Pb [37, 38], and with other determinations of the so-called ‘neutron skin’.

3. Results

Following the optical potential approach described in the preceding section, and more extensively in Refs. [19, 26], global fits to strong-interaction level shifts and widths from Ne to U were made over a wide range of values for the neutron-skin parameter γ as shown in Fig. 2.

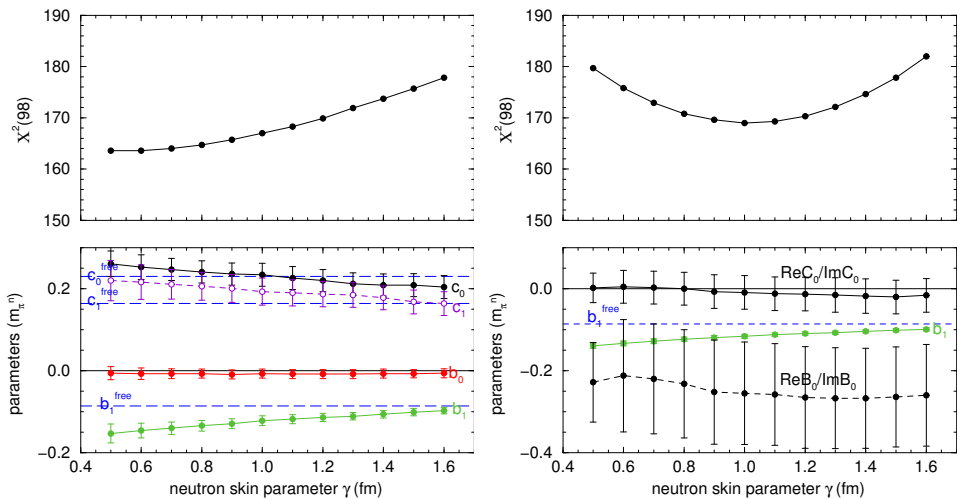


Fig. 2. Fits to 98 pionic atoms data points for $\sigma_{\pi N} = 0$ as a function of the neutron-skin parameter γ , with χ^2 values plotted in the upper panels and fitted values of some of the π -nucleus optical potential parameters plotted in the lower panels. No χ^2 minimum is reached in the 8-parameter left-panel fits, but fixing the p-wave parameters c_0 and c_1 at their SAID [39] threshold values 0.23 and 0.16 m_π^{-3} , respectively, produces the fits shown in the right panels.

The fitted 98 data points include ‘deeply bound’ states in Sn isotopes and in ^{205}Pb . Varying all eight parameters (real b_0, b_1, c_0, c_1 ; complex B_0, C_0) in Eqs. (10)–(12) produces good χ^2 fits, $\chi^2 \sim 170$, but short of a well-defined $\chi^2(\gamma)$ minimum as clearly seen in the upper left panel of Fig. 2. The lower left panel shows that the single-nucleon parameters are well-determined and vary smoothly with γ .

Holding the p-wave single-nucleon parameters c_0, c_1 fixed at their SAID free-space threshold values marked by dashed horizontal lines, thereby reducing the number of fitted parameters to six, a χ^2 minimum around $\gamma = 1$ to 1.1 fm was reached as shown in the upper right panel of Fig. 2. In these six-parameter fits, $\text{Im } B_0$ and $\text{Im } C_0$ (not shown) come out well-determined, with values almost independent of γ , but $\text{Re } B_0$ and $\text{Re } C_0$ are poorly determined as seen in the lower right panel of the figure. In all the fits shown here in Fig. 2, b_1 was treated as a free parameter regardless of any possible functional dependence on $\sigma_{\pi N}$, thereby corresponding to $\sigma_{\pi N} = 0$ in Eq. (14). The fitted values of b_1 disagree then over a broad range of γ s with the value b_1^{free} marked by a dashed horizontal line.

Introducing the in-medium density dependence of b_1 given by Eq. (14) in terms of $\sigma_{\pi N}$, we first demonstrate the effect of using a fixed value of $\sigma_{\pi N} = 50$ MeV, as practised in all of our past works [26], on the fitted parameters. This is shown within six-parameter fits in the left panels of Fig. 3. Rather than keeping the p-wave single-nucleon parameters c_0 and c_1 to their SAID free-space threshold values, as done in the $\sigma_{\pi N} = 0$ fits shown in the right panels of Fig. 2, here we kept $\text{Re } B_0$ and $\text{Re } C_0$ at zero values thereby producing as good fits to the data as by letting them vary. In particular, suppressing $\text{Re } B_0$ in pionic atoms fits amounts to absorbing it into an effective b_0 parameter [31]. The fitted c_0 and c_1 , particularly c_0 , are clearly seen in the lower panel to come out close to the respective free-space values. As for the s-wave single-nucleon parameters b_0 and b_1 , the dominance of b_1 with respect to b_0 is also clearly seen. The introduction of a nonzero value of $\sigma_{\pi N}$ allows b_1 to reach its free-space value b_1^{free} beginning at a neutron-skin parameter γ value of 1.1 fm.

Holding now the p-wave single-nucleon parameters c_0 and c_1 at their free-space SAID threshold values 0.23 and $0.16 m_\pi^{-3}$, respectively, and keeping as before $\text{Re } B_0$ and $\text{Re } C_0$ at zero values, we show in the right panels of Fig. 3 four-parameter fits where the varied parameters are $b_0, \sigma_{\pi N}$ for b_1 using Eq. (6), $\text{Im } B_0$ and $\text{Im } C_0$. A minimum value of $\chi_{\text{min}}^2 = 167.1$ is reached at $\gamma \approx 1.1$ fm, where $\sigma_{\pi N}$ assumes a value of $\sigma_{\pi N}^{\text{FG}} = 56.9 \pm 6.9$ MeV. Note that a value of $\gamma \approx 1.1$ fm agrees with other determinations of this quantity in ^{208}Pb [38]. To check the dependence of $\sigma_{\pi N}$ on b_0 , we repeated fits with b_0 kept fixed at either one of the two free-space threshold values listed in Eq. (3), varying then also $\text{Re } B_0$ and $\text{Re } C_0$. Typical χ^2 values increased by 20 to 30,

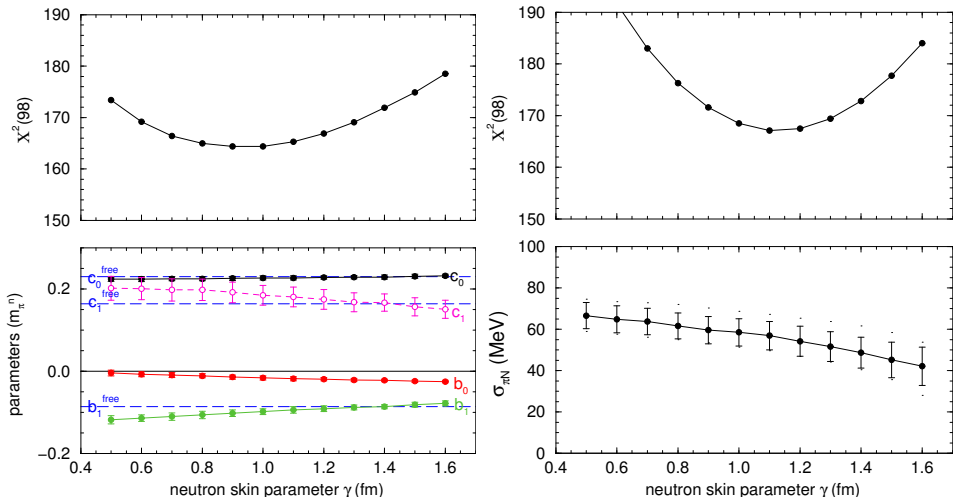


Fig. 3. Left: 6-parameter fits with $\sigma_{\pi N} = 50$ MeV, where $\text{Re } B_0$ and $\text{Re } C_0$ are kept zero. Right: 4-parameter fits where c_0 and c_1 , additionally, are kept at their SAID [39] threshold values 0.23 and $0.16 m_\pi^{-3}$, respectively. Of the 4 varied parameters (b_0 , b_1 , $\text{Im } B_0$, $\text{Im } C_0$) b_1 is related to $\sigma_{\pi N}$ by Eq. (6). Resulting values of $\sigma_{\pi N}$ are plotted in the lower right panel.

but the χ^2 minima remained at $\gamma = 1.1$ to 1.2 fm with corresponding values of $\sigma_{\pi N}$ decreasing at most by 3 MeV. We also note that the resulting value of $\sigma_{\pi N}$ is identical with that derived in our recently published work [18] where the effect on the derived value of $\sigma_{\pi N}$ of form-factor folding, $\rho_{n,p} \rightarrow \tilde{\rho}_{n,p}$ in the p-wave terms (11), (12) of the pion–nucleus optical potential, was shown to be negligibly small.

4. Discussion and summary

The pionic atoms fits and the value of the πN σ term $\sigma_{\pi N}$ extracted in the present work are based on the in-medium renormalization of the near-threshold πN isovector scattering amplitude b_1 as given by Eq. (6), derived at LO from Eqs. (4) and (5) for the in-medium decrease of the pion decay constant f_π associated via the GMOR expression with the in-medium decrease of the quark condensate $\langle \bar{q}q \rangle$. Higher order corrections to this simple form have been proposed in the literature and were discussed by us in Ref. [18]. Briefly, one may classify two such corrections arising from: (i) NN correlation contributions [40] from one- and two-pion interaction terms, increasing the fitted $\sigma_{\pi N}$ value by about 7 MeV (or by a smaller amount following a chiral approach at NLO [41]); and (ii) an upward shift of the in-medium pion mass $m_\pi(\rho)$ in symmetric nuclear matter from its

free-space value [42], decreasing the fitted $\sigma_{\pi N}$ value by a similar amount, and also by adding corrections of the order of $\rho^{4/3}$ [43, 44] which at a typical nuclear density $\rho_{\text{eff}} = 0.1 \text{ fm}^{-3}$ [31] are negligible. Interestingly but perhaps fortuitously, these two higher-order effects largely cancel each other.

In conclusion, we have derived in this work a value of $\sigma_{\pi N}^{\text{FG}} = 57 \pm 7 \text{ MeV}$ from a large scale fit to pionic atoms observables, in agreement with the relatively high $\sigma_{\pi N}$ values reported in recent studies based on modern hadronic πN phenomenology [6], but in disagreement with the considerably lower $\sigma_{\pi N}$ values reached in some of the recent modern lattice QCD calculations, *e.g.* [12]. Our derivation is based on the model introduced by Weise and collaborators [24, 25, 34] for the in-medium renormalization of the πN near-threshold isovector scattering amplitude, using its leading density dependence Eq. (6), and was found robust in fitting the wealth of pionic atoms data against variation of other πN interaction parameters that enter the low-energy pion self-energy operator. The two types of model corrections beyond the leading density dependence considered here were found to be relatively small, a few MeV each, and partly canceling each other. Further model studies are desirable in order to confirm this conclusion.

We are grateful to Norbert Kaiser, Wolfram Weise and Nodoka Yamanaka for useful correspondence on the subject of the present work.

REFERENCES

- [1] M.E. Sainio, *πN Newslett.* **16**, 138 (2002) [arXiv:hep-ph/0110413].
- [2] J.M. Alarcón, J.M. Camalich, J.A. Oller, *Phys. Rev. D* **85**, 051503 (2012).
- [3] Y.-H. Chen, D.-L. Yao, H.Q. Zheng, *Phys. Rev. D* **87**, 054019 (2013).
- [4] M. Hoferichter, J. Ruiz de Elvira, B. Kubis, U.-G. Meißner, *Phys. Rev. Lett.* **115**, 092301 (2015).
- [5] V. Dmitrašinović, H.-X. Chen, A. Hosaka, *Phys. Rev. C* **93**, 065208 (2016).
- [6] J. Ruiz de Elvira, M. Hoferichter, B. Kubis, U.-G. Meißner, *J. Phys. G* **45**, 024001 (2018).
- [7] R. Horsley *et al.* [QCDSF-UKQCD Collab.], *Phys. Rev. D* **85**, 034506 (2012).
- [8] S. Durr *et al.* [BMW Collab.], *Phys. Rev. Lett.* **116**, 172001 (2016).
- [9] Y.-B. Yang, A. Alexandru, T. Draper, K.-F. Liu [χ QCD Collab.], *Phys. Rev. D* **94**, 054503 (2016).
- [10] A. Abdel-Rehim *et al.* [ETM Collab.], *Phys. Rev. Lett.* **116**, 252001 (2016).
- [11] G.S. Bali *et al.* [RQCD Collab.], *Phys. Rev. D* **93**, 094504 (2016).
- [12] N. Yamanaka, S. Hashimoto, T. Kaneko, H. Ohki [JLQCD Collab.], *Phys. Rev. D* **98**, 054516 (2018).

- [13] C. Alexandrou *et al.* [ETM Collab.], [arXiv:1909.00485](https://arxiv.org/abs/1909.00485) [hep-lat].
- [14] D.B. Leinweber, A.W. Thomas, S.V. Wright, *Phys. Lett. B* **482**, 109 (2000).
- [15] L. Alvarez-Ruso, T. Ledwig, J.M. Camalich, M.J. Vicente-Vacas, *Phys. Rev. D* **88**, 054507 (2013).
- [16] X.-L. Ren, L.-S. Geng, J. Meng, *Phys. Rev. D* **91**, 051502(R) (2015).
- [17] X.-L. Ren, X.-Z. Ling, L.-S. Geng, *Phys. Lett. B* **783**, 7 (2018).
- [18] E. Friedman, A. Gal, *Phys. Lett. B* **792**, 340 (2019).
- [19] E. Friedman, A. Gal, *Phys. Rep.* **452**, 89 (2007).
- [20] M. Hoferichter, J. Ruiz de Elvira, B. Kubis, U.-G. Meißner, *Phys. Lett. B* **760**, 74 (2016).
- [21] V. Baru *et al.*, *Phys. Lett. B* **694**, 473 (2011); *Nucl. Phys. A* **872**, 69 (2011).
- [22] Y. Tomozawa, *Nuovo Cim. A* **46**, 707 (1966); S. Weinberg, *Phys. Rev. Lett.* **17**, 616 (1966).
- [23] M. Gell-Mann, R.J. Oakes, B. Renner, *Phys. Rev.* **175**, 2195 (1968).
- [24] W. Weise, *Acta Phys. Pol. B* **31**, 2715 (2000).
- [25] W. Weise, *Nucl. Phys. A* **690**, 98c (2001).
- [26] E. Friedman, A. Gal, *Nucl. Phys. A* **928**, 128 (2014) and references therein to earlier work on pionic atoms.
- [27] E. Friedman *et al.*, *Phys. Rev. Lett.* **93**, 122302 (2004).
- [28] E. Friedman *et al.*, *Phys. Rev. C* **72**, 034609 (2005).
- [29] M. Ericson, T.E.O. Ericson, *Ann. Phys.* **36**, 323 (1966).
- [30] A. Gal, H. Garcilazo, *Nucl. Phys. A* **864**, 153 (2011), in particular Fig. 2 and Table 3.
- [31] R. Seki, K. Masutani, *Phys. Rev. C* **27**, 2799 (1983).
- [32] M. Krell, T.E.O. Ericson, *Nucl. Phys. B* **11**, 521 (1969).
- [33] N. Kaiser, W. Weise, *Phys. Lett. B* **512**, 283 (2001).
- [34] E.E. Kolomeitsev, N. Kaiser, W. Weise, *Phys. Rev. Lett.* **90**, 092501 (2003).
- [35] H. Geissel *et al.*, *Phys. Lett. B* **549**, 64 (2002); *Phys. Rev. Lett.* **88**, 122301 (2002).
- [36] E. Friedman, *Hyperfine Interact.* **193**, 33 (2009).
- [37] E. Friedman, *Nucl. Phys. A* **896**, 46 (2012).
- [38] C.M. Tarbert *et al.*, *Phys. Rev. Lett.* **112**, 242502 (2014).
- [39] R.A. Arndt, W.J. Briscoe, I.I. Strakovsky, R.L. Workman, *Phys. Rev. C* **74**, 045205 (2006); evolving SAID program <http://gwdac.physics.gwu.edu/>
- [40] N. Kaiser, P. de Homont, W. Weise, *Phys. Rev. C* **77**, 025204 (2008).
- [41] A. Lacour, J.A. Oller, U.-G. Meißner, *J. Phys. G* **37**, 125002 (2010).
- [42] D. Jido, T. Hatsuda, T. Kunihiro, *Phys. Lett. B* **670**, 109 (2008).
- [43] S. Goda, D. Jido, *Phys. Rev. C* **88**, 065204 (2013).
- [44] S. Goda, D. Jido, *Prog. Theor. Exp. Phys.* **2014**, 033D03 (2014).